

Transactions Briefs

Low-Frequency Differentiators and Integrators for Biomedical and Seismic Signals

Mohamad Adnan Al-Alaoui

Abstract—A general active-network synthesis approach to inverse system design is introduced. The approach is applied to a passive RC differentiator and a passive RC integrator to obtain, respectively, a very low-frequency differential integrator and a very low-frequency differential differentiator. The frequency ranges of the proposed circuits, from dc to a few hundred hertz, are particularly suitable to the frequency ranges of biomedical and seismic signals. The advantages of the proposed circuits are delineated and include single time constants, dc stable integrators, and resistive input differentiators. Noninverting and inverting differentiators and integrators could be obtained by grounding one of the input terminals in the differential configurations.

Index Terms—Active-network synthesis, biomedical signals, differentiators, integrators, inverse system design, low frequency, seismic signals.

I. INTRODUCTION

This paper introduces a differential integrator and a differential differentiator for the very low-frequency signals, from dc to a few hundred hertz, that arise in the measurements of biomedical signals [1] and seismic signals [2]. The resulting low-frequency integrators and differentiators are eminently suitable for use with biomedical and seismic signals where the conventional wisdom advises us to seek DSP solutions for such low frequencies, because they are deemed to be not practically attainable by using analog filters [2]. The analog filters are often simpler to implement and do not require the possible added complexity and cost of analog-to-digital and digital-to-analog converters.

The basic concept of both circuits is to employ an inverse system design to obtain the inverse of a passive RC integrator and a passive RC differentiator which yield, respectively, active RC differentiator, and integrator [3]–[6]. The traditional differential integrator and differential differentiator are shown in Figs. 1 and 2, respectively [7].

The proposed circuits have the following advantages over the traditional circuits.

- 1) Single time constants are obtained for both circuits.
- 2) Resistive inputs, without using input buffers, are obtained for both circuits.
- 3) The integrator is dc stable and the differentiator action ceases at high frequencies.
- 4) Reasonably high-quality integration and differentiation can be obtained while avoiding the dc instability for the integrator and the instability caused by the capacitive input of the differentiator.
- 5) It is easier to control the common-mode rejection ratio (CMRR) with a single time constant, by choosing appropriately small tolerance resistances and an appropriate amplifier.

Manuscript received March 9, 2000; revised January 24, 2001, and February 27, 2001. This work was supported in part by the University Research Board of the American University of Beirut. This paper was recommended by Associate Editor N. M. K. Rao.

The author is with the Department of Electrical and Computer Engineering, American University of Beirut, Beirut 1107–2020, Lebanon.

Publisher Item Identifier S 1057-7122(01)06083-4.

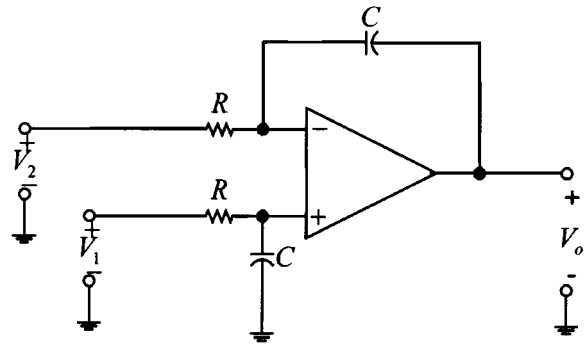


Fig. 1. The traditional differential integrator.

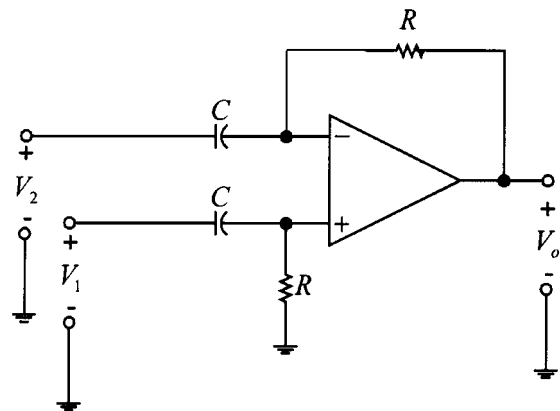


Fig. 2. The traditional differential differentiator.

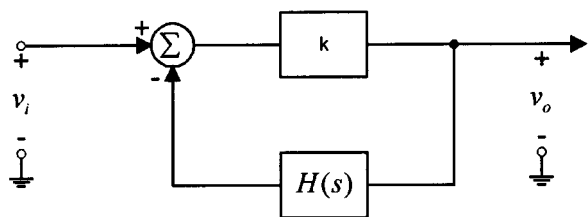


Fig. 3. A block diagram of inverse system design.

- 6) Functional-bandpass integrators and differentiators are obtained with control over both frequency limits of the bandpass. The limited bandwidth mitigates the noise contribution.

II. THE BASIC CONCEPT: ACTIVE NETWORK SYNTHESIS OF INVERSE SYSTEM DESIGN

The basic concept came from observing that the inverse of a passive RC differentiator approximates the ideal integrator. Also the inverse of a passive RC integrator approximates an ideal differentiator.

The approach to inverse-system synthesis is shown in Fig. 3. The transfer function relating the output voltage to the input voltage of Fig. 3 is [3]–[5]

$$\frac{V_o(s)}{V_i(s)} = \frac{k}{1 + kH(s)}. \quad (1)$$

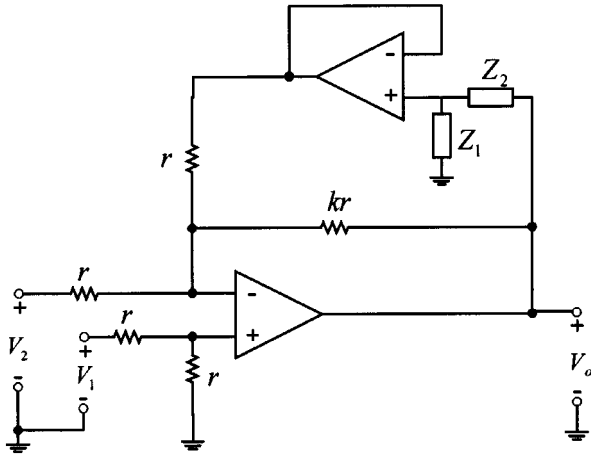


Fig. 4. The proposed active-network synthesis of inverse system design.

The system will approximate $1/H(s)$ in the frequency range where

$$kH(s) \gg 1. \quad (2)$$

The proposed approach to active-network synthesis, with dual-input configuration, is shown in Fig. 4. The open-loop transfer function of the operational amplifier used in the differential stage will be denoted as $A(s)$ while the one used in the buffer stage, implemented as an isolation amplifier, will be designated as $A_B(s)$. The transfer function relating the output voltage of the isolation-stage operational amplifier to its input can be shown to be $1/[(1/A_B(s)) + 1] \approx 1$ for low frequencies. It should be noted that the isolation amplifier can be dispensed with if r is chosen large enough such that the loading of the circuit composed of Z_1 and Z_2 is negligible. The derivation of the transfer function of the differential circuit of Fig. 4, relating its output voltage to its input voltage, is outlined in the following.

Let V^- , V^+ , and V_X designate the voltages in Fig. 4, with respect to ground, from the inverting terminal of the integrator stage operational amplifier, the noninverting terminal of the operational amplifier to ground and the voltage across the Z_1 impedance, respectively.

Nodal analysis, similar to those which were carried out in [3]–[6], assuming that the output voltage of the isolation amplifier has the value V_X and that for the low-frequency range $A(s)$ is very large, $|A(s)| \gg k$, and $k \gg 1$, yields

$$\frac{V_o}{V_1 - V_2} \approx \frac{k(Z_1 + Z_2)}{kZ_1 + Z_2}. \quad (3)$$

In the limit if k is infinite, which corresponds to removing the feedback resistor labeled kr in Fig. 5, (3) simplifies further to

$$\frac{V_o}{V_1 - V_2} \approx \frac{(Z_1 + Z_2)}{Z_1}. \quad (4)$$

The system might still be stable, since there remains a feedback path through the isolation amplifier. The stability will depend on Z_1 and Z_2 and should be investigated for each case separately.

III. THE PROPOSED LOW-FREQUENCY DIFFERENTIAL INTEGRATOR

A. The Derivation of the Transfer Function

The derivation of the transfer function of the proposed differential integrator of Fig. 5, relating its output voltage to its input voltage, is outlined in the following.

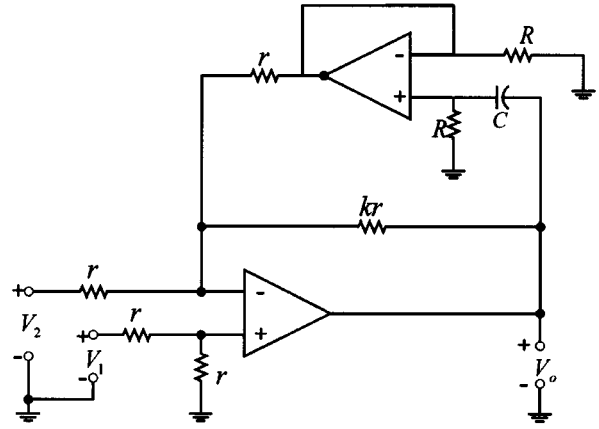


Fig. 5. The proposed low-frequency differential integrator.

Fig. 5 is obtained from Fig. 4 with $Z_1 = R$ and $Z_2 = 1/Cs$. Hence (3) yields

$$\frac{V_o}{V_1 - V_2} \approx \frac{k(1 + RC's)}{1 + kRCs}. \quad (5)$$

If $RCs \ll 1$, or equivalently $\omega \ll 1/(RC)$, (5) simplifies to

$$\frac{V_o}{V_1 - V_2} \approx \frac{k}{1 + kRCs}. \quad (6)$$

Equation (6) represents an integrator for the frequencies in the range

$$\frac{1}{kRC} \ll \omega \ll \frac{1}{RC}. \quad (7)$$

The circuit acts as an amplifier for dc inputs. The dc gain is obtained from (6) by substituting zero for s to obtain the dc value of k . Thus, the dc gain may be increased or decreased as desired by respectively increasing or decreasing k . Note that the resulting dc stability is one of the advantages of the circuit over the traditional Miller integrator, which is dc unstable due to the high gain, A_o , of the operational amplifier. Typically $A_o \approx 10^5$ for LM 741 operational amplifier.

B. The Quality Factor Q of the Differential Integrator

If we express the transfer function of an integrator as [3]–[5]

$$T(j\omega) = \frac{1}{R(\omega) + jX(\omega)} \quad (8)$$

then, the Q -factor of the integrator is defined as

$$Q = \frac{X(\omega)}{R(\omega)}. \quad (9)$$

The traditional differential integrator, with a Q value equal to that of the Miller integrator, has $Q = -|A| = -|\omega_c/s| = -|\omega_c/\omega|$.

For the ideal or low-frequency case, we obtain, from (6), the value

$$Q = kRC\omega \gg 1. \quad (10)$$

Thus, for $RC\omega = 0.1$ and $k = 1000$, we obtain a Q value of 100.

C. The Case of Infinite k

Note that (6) represents a stable system, with its pole in the left half of the s -plane. In the limit, if k is infinite, the right hand side of (6) will simplify to $1/RCs$ which has a pole at the origin and the system will not be stable. However, if the capacitance is shunted with a resistor, the

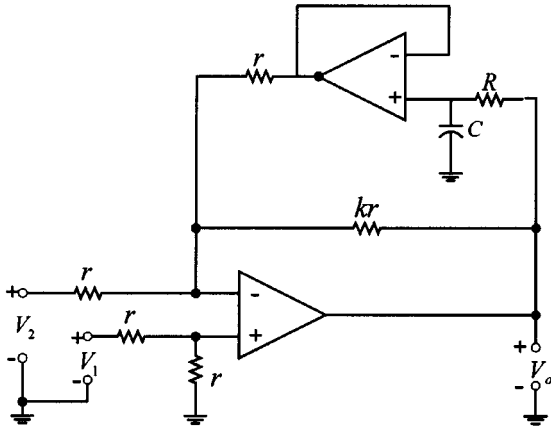


Fig. 6. The proposed low-frequency differential differentiator.

resulting system will be stable and will still act as an integrator. In this case, let $Z_1 = R_1$ and $Z_2 = R_2/(1 + R_2Cs)$. Thus, we will have

$$\frac{V_o}{V_1 - V_2} \approx \frac{(R_1 + R_2) \left(1 + \frac{R_1 R_2}{R_1 + R_2} Cs\right)}{R_1(1 + R_2Cs)}. \quad (11)$$

Equation (11) represents a stable and a minimum phase system, with a single pole and a single zero in the left half of the s plane. It can be verified that the above circuit acts as an integrator in the frequency range

$$\frac{1}{R_2C} \ll \omega \ll \frac{1}{R_2C} + \frac{1}{R_1C}. \quad (12)$$

For brevity, this case will not be further elaborated.

IV. PROPOSED LOW-FREQUENCY DIFFERENTIAL DIFFERENTIATOR

A. The Derivation of the Transfer Function

The derivation of the transfer function of the differential differentiator of Fig. 6, relating its output voltage to its input voltage, is outlined in the following.

In this case, Fig. 6 is obtained from Fig. 4 with $Z_1 = 1/Cs$ and $Z_2 = R$, hence (3) yields

$$\frac{V_o}{V_1 - V_2} \approx \frac{k(1 + RC's)}{k + RCs}. \quad (13)$$

Equation (13) represents a differentiator for frequencies in the range

$$\frac{1}{RC} \ll \omega \ll \frac{k}{RC}. \quad (14)$$

Indeed in the frequency range specified by (14), (13) can be approximated as

$$\frac{V_o}{V_1 - V_2} \approx RC's. \quad (15)$$

The circuit acts as an amplifier for dc inputs. The dc gain is obtained from (13) by substituting zero for s to obtain a dc gain of ≈ 1 .

B. The Quality Factor Q of the Differential Differentiator

If we express the transfer function of a differentiator as [6]

$$T(j\omega) = R(\omega) + jX(\omega) \quad (16)$$

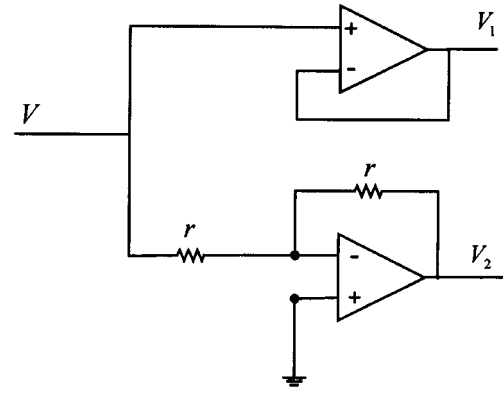


Fig. 7. The simulation and experimental setup used to obtain equal voltages of opposite polarities. Both operational amplifiers are LM741 and $r = 10 \text{ k}\Omega$.

then the Q -factor of the differentiator is defined as

$$Q = \frac{X(\omega)}{R(\omega)}. \quad (17)$$

The traditional differential differentiator, with a Q value equal to that of the Miller integrator, has $Q = -|A| = -|\omega_c/s| = -|\omega_c/\omega|$.

For the ideal or low-frequency case, we obtain, from (13), with $RCs \gg 1$, the value

$$Q = k/RC\omega. \quad (18)$$

Thus for $RC\omega = 1$ and $k = 100$, we obtain a Q value of 100.

C. The Case of Infinite K

Note that for an infinite k the right hand side of (13) reduces to $(1 + RCs)$ and the system is still a stable system. Thus the feedback resistor could be removed and the range of frequency is $\omega \gg 1/(RC)$. The differentiator is no longer confined to the low-frequency range. The high frequency range of the differentiator is limited by the gain-bandwidth characteristics of the operational amplifier. For brevity, this case will not be further elaborated.

V. SIMULATION AND EXPERIMENTAL RESULTS

A. Obtaining Two Voltages of Opposite Polarities and Equal Magnitudes

The circuit of Fig. 7 was used in all the simulation and experimental work. Voltages of opposite polarities, and with roughly equal delay and magnitude, are obtained from the outputs of the two LM741 operational amplifiers in Fig. 7, upon the application of a voltage at the input terminals designated as V . One of the operational amplifiers is configured as an inverting amplifier with a gain of -1 , while the other is configured as a unity gain voltage-follower amplifier. The output of the voltage follower was connected to the inputs designated as V_1 in Figs. 5 and 6, while the output of the inverting amplifier was connected to the inputs designated as V_2 in Figs. 5 and 6.

B. The Simulation Results

The differential integrator circuit of Fig. 5 was simulated by using PSPICE with $r = 100 \text{ k}\Omega$, $k = 1000$, $C = 100 \text{ }\mu\text{F}$, $R = 100 \text{ k}\Omega$ and LM741 for the operational amplifier with dc bias of $\pm 15 \text{ V}$. The simulation results for the magnitude and phase are shown in Fig. 8. The simulation shows that, with the above values, the circuit acts as an integrator for the low-frequency range in the neighborhood of 1 mHz, in agreement with (7). Different frequency ranges may be obtained by varying R and/or C appropriately.

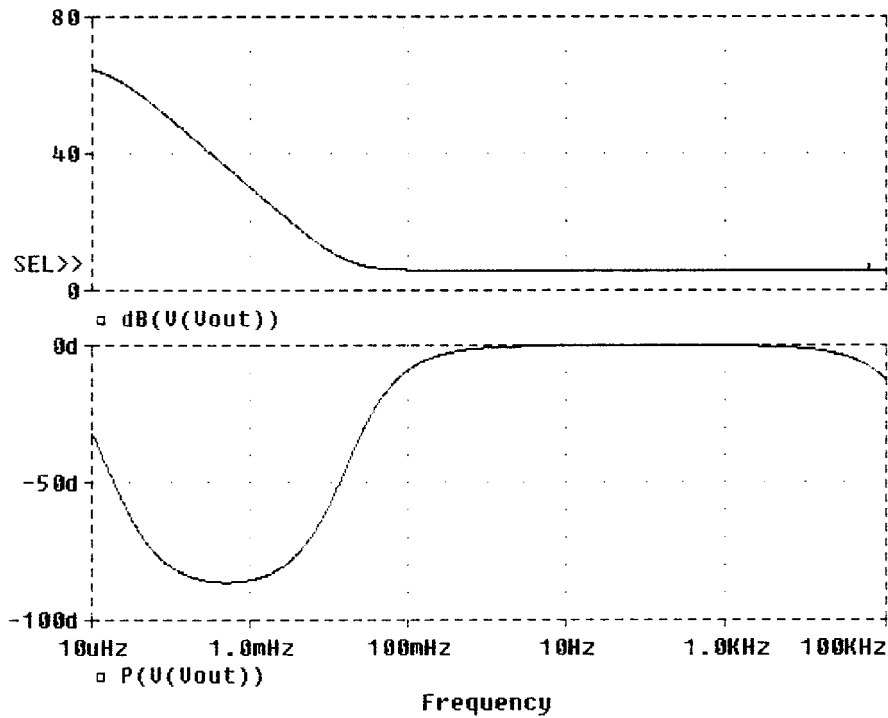


Fig. 8. PSPICE Simulation of the proposed differential integrator.

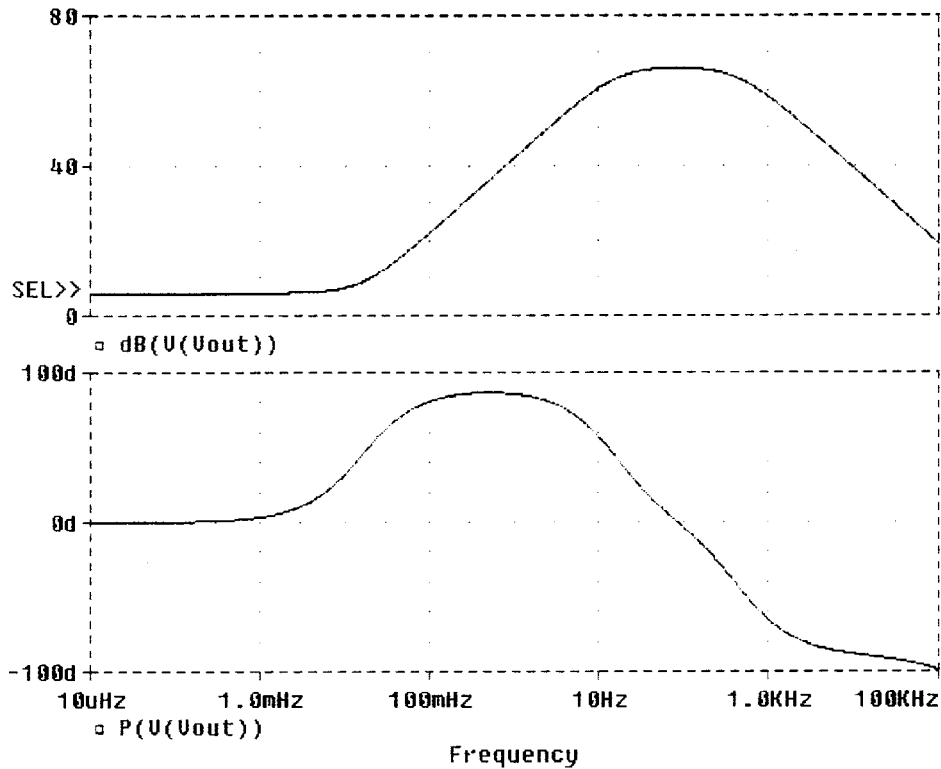


Fig. 9. PSPICE Simulations of the proposed differential differentiator.

The differential differentiator circuit of Fig. 6 was simulated by using PSPICE with $r = 100\text{ k}\Omega$, $k = 1000$, $C = 100\text{ }\mu\text{F}$, $R = 100\text{ K}\Omega$ and LM741 for the operational amplifier with dc bias of $\pm 15\text{ V}$. The simulation results for the magnitude and phase are shown in Fig. 9. The simulation shows that, with the above values, the circuit acts as a differentiator for the low-frequency range in the neighborhood of 1 Hz,

in agreement with (14). Different frequency ranges may be obtained by varying R and/or C appropriately.

C. The Experimental Results

The experimental set up utilized, in addition to the circuit of Fig. 7 and the circuit being tested corresponding to Fig. 5 or Fig. 6, a power

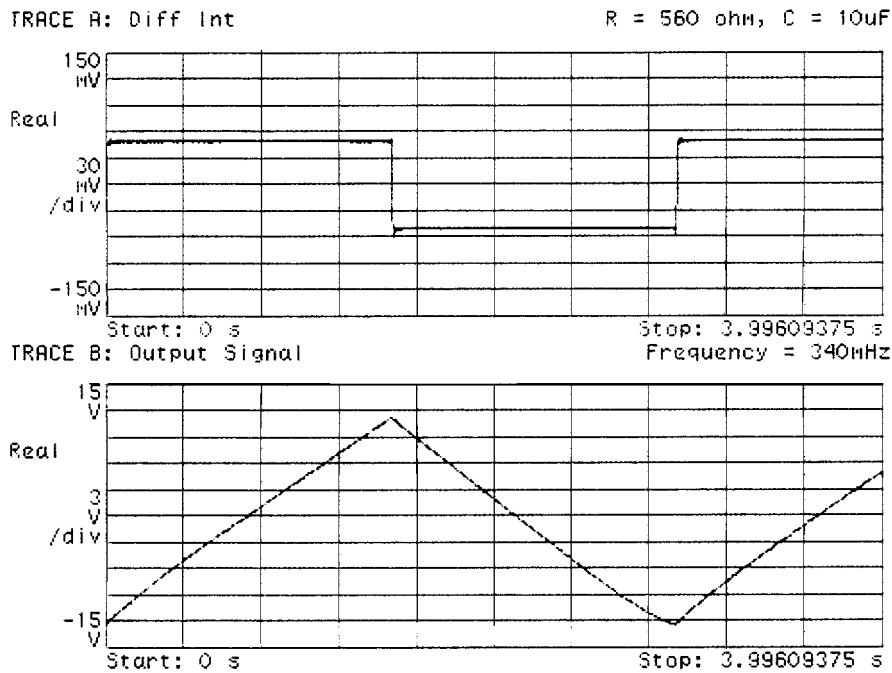


Fig. 10. Experimental results of the differential integrator, where the upper trace is the rectangular input waveform and the bottom trace is the triangular output waveform.

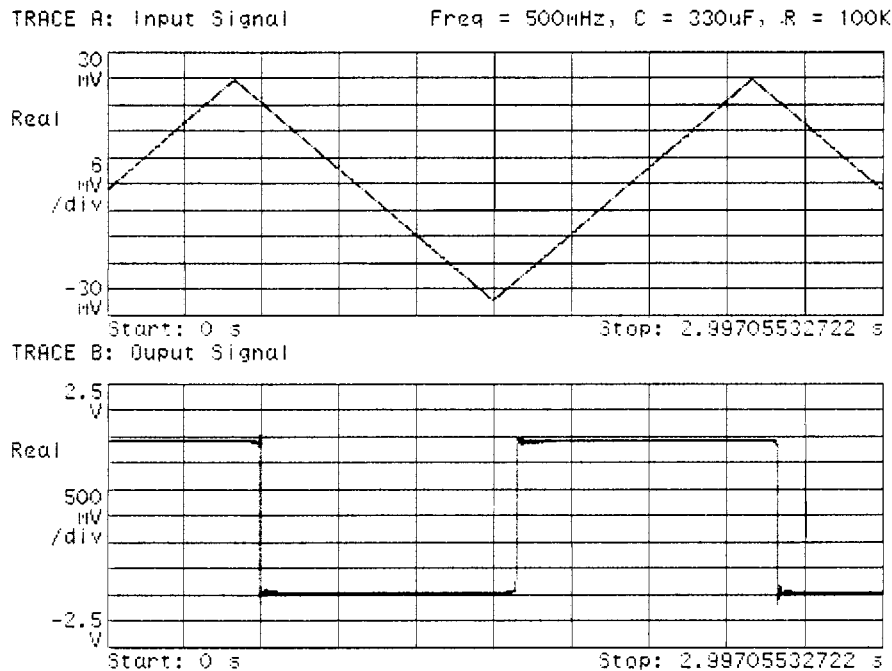


Fig. 11. Experimental results of the differential differentiator, where the upper trace is the triangular input waveform and the bottom trace is the rectangular output waveform.

supply to provide the dc bias of ± 15 V, function generator HP33120 which provided rectangular wave voltages to the inputs of the integrator circuit and triangular wave voltages to the input of the differentiator circuit, and signal analyzer HP89410A which provided the displays of the input and output waveforms shown in Figs. 10 and 11.

Fig. 10 shows the experimental results of the differential integrator of Fig. 5, with $r = 100$ k Ω , $k = 1000$, $C = 10$ μ F, $R = 560$ Ω and LM741 for the operational amplifier with dc bias of ± 15 V. The upper trace shows the input square waveform with a frequency of 340 mHz. The bottom trace shows the resulting triangular waveform at the output

of the operational amplifier. Thus, a good integration action is obtained by using the proposed circuit. Note that in Fig. 5 the addition of resistor of value $R = 560$ Ω between the negative input terminal of the isolation operational amplifier and ground was necessary to ameliorate the offset voltage at the output. Keeping the same value of the resistance seen from each of the two input terminals of the operational amplifiers to ground reduces the offset voltage at the output since the values of the dc currents into the two terminals are almost equal.

Fig. 11 shows the experimental results of the differential differentiator of Fig. 6, with $r = 100$ k Ω , $k = 1000$, $C = 330$ μ F, $R = 100$

$k\Omega$ and LM741 for the operational amplifier with dc bias of ± 15 V. The upper trace shows the input triangular waveform with a frequency of 500 mHz. The bottom trace shows the rectangular waveform at the output of the operational amplifier. Thus, a good differentiation action is obtained by using the proposed circuit. It was not necessary to add a resistor between the negative input terminal of the isolation operational amplifier and ground since a dc input to a differentiator produces a zero output voltage.

D. Comparison Among the Theoretical, Simulation, and Experimental Results

The simulation and experimental results verify the predicted frequency ranges of (7) for the integrator and (14) for the differentiator. Note also that the clean waveforms of Figs. 10 and 11 indicate high signal to noise ratios for both circuits.

It should be pointed out that the case of infinite k , with the feedback resistor kr removed, produced good experimental and simulation results which were omitted for brevity.

VI. CONCLUSION

An active-network synthesis of inverse system design is presented. The synthesis is general and can be applied with different impedances. Its application to invert a passive differentiator resulted in a versatile low-frequency differential integrator. Its application to invert a passive RC integrator yielded a versatile low-frequency differential differentiator. Each employs a single time constant, has a resistive input, and a reasonably high Q value. Simulation and experimental results verify the theoretical expectations. The active-network synthesis can be applied to obtain other varied realizations. The differential integrators and differentiators could easily be modified to obtain inverting and non-inverting integrators and differentiators by simply grounding one of the two inputs in each of the differential configurations. Additionally, the limited bandwidths of the circuits mitigates the contribution of the noise and yield output waveforms with large signal to noise ratios.

ACKNOWLEDGMENT

The author wishes to thank S. K. Mitra for providing the atmosphere conducive to research by inviting him to spend the summer of 1997 at the Signal and Image Processing Laboratory of University of California at Santa Barbara, where this research was initiated, and R. Ferzli, F. El-Zoghet, F. Elias, and B. Alawieh for their help in the production of the figures, simulation, and experimental results.

REFERENCES

- [1] W. J. Tompkins and J. G. Webster, Eds., *Design of Microcomputer-Based Medical Instrumentation*. Englewood Cliffs, NJ: Prentice-Hall, 1981.
- [2] S. K. Mitra, *Digital Signal Processing*, 2nd ed. New York: McGraw-Hill, 2001.
- [3] M. A. Al-Alaoui, "A novel approach to designing a noninverting integrator with built-in low-frequency stability, high-frequency compensation and high Q ," *IEEE Trans. Instrum. Meas.*, vol. 38, pp. 1116–1121, Dec. 1989.
- [4] —, "A stable inverting integrator with an extended high-frequency range," *IEEE Trans. Circuits Syst. II*, vol. 45, pp. 399–402, Mar. 1998.
- [5] —, "A differential integrator with a built-in high frequency compensation," *IEEE Trans. Circuits Syst. I*, vol. 45, pp. 517–522, May 1998.
- [6] —, "A novel differential differentiator," *IEEE Trans. Instrum. Meas.*, vol. 40, pp. 826–830, Oct. 1991.
- [7] J. G. Graeme, *Applications of Operational Amplifiers*. Tokyo, Japan: McGraw-Hill, 1973.

Robust Stabilization of Singular-Impulsive-Delayed Systems With Nonlinear Perturbations

Zhi-Hong Guan, C. W. Chan, Andrew Y. T. Leung, and Guanrong Chen

Abstract—Many dynamic systems in physics, chemistry, biology, engineering, and information science have impulsive dynamical behaviors due to abrupt jumps at certain instants during the dynamical process, and these complex dynamic behaviors can be modeled by singular impulsive differential systems. This paper formulates and studies a model for singular impulsive delayed systems with uncertainty from nonlinear perturbations. Several fundamental issues such as global exponential robust stabilization of such systems are established. A simple approach to the design of a robust impulsive controller is then presented. A numerical example is given for illustration of the theoretical results. Meanwhile, some new results and refined properties associated with the M -matrices and time-delay dynamic systems are derived and discussed.

Index Terms—Impulsive systems, nonlinear perturbation, robust stabilization, singular systems, time-delay, uncertainty.

I. INTRODUCTION

In recent years, considerable efforts have been devoted to the analysis and synthesis of singular systems (known also as descriptor systems, semistate systems, differential algebraic systems, generalized state-space systems, etc.). These systems arise naturally in various fields including electrical networks [25], robotics [22], [23], social, biological, and multisector economic systems [21], [29], dynamics of thermal nuclear reactors [26], automatic control systems [27], among many others such as singular perturbation systems. Progress in the investigation of singular systems can be found in books [1], [4], [6], [8] and survey papers [5], [15], [16].

Although most singular systems are analyzed either in the continuous- or discrete-time setting, many singular systems exhibit both continuous-time and discrete-time behaviors. Examples include many evolutionary processes, especially those in biological systems such as biological neural networks and bursting rhythm models in pathology. Other examples exist in optimal control of economic systems, frequency-modulated signal processing systems, and some flying object motions. These systems are characterized by abrupt changes in the states at certain instants [3], [9], [10], [11], [14]. This type of impulsive phenomena can also be found in the fields of information science, electronics, automatic control systems, computer networks, artificial intelligence, robotics, and telecommunications [10]. Many sudden and sharp changes occur instantaneously in singular systems, in the form of impulses which cannot be well described by a pure continuous-time or discrete-time model. For instance, if the initial conditions is inconsistent, then a singular system will have a finite

Manuscript received September 11, 2000. This work was supported in part by the National Natural Science Foundation of China under Grant 69774038 and Grant 60074009, in part by the Doctorate Foundation of the Education Ministry of China under Grant 199048718, and in part by the Foundation for University Key Teacher, Education Ministry of China. This paper was recommended by Associate Editor M. Gilli.

Z.-H. Guan is with the Department of Control Science and Engineering, Huazhong University of Science and Technology, Wuhan, Hubei, 430074, China.

C. W. Chan is with the Department of Mechanical Engineering, The University of Hong Kong, Pokfulam Road, Hong Kong.

A. Y. T. Leung is with the Department of Building and Construction, City University of Hong Kong, Kowloon, Hong Kong.

G. Chen is with the Department of Electronic Engineering, City University of Hong Kong, Kowloon, Hong Kong.

Publisher Item Identifier S 1057-7122(01)06082-2.